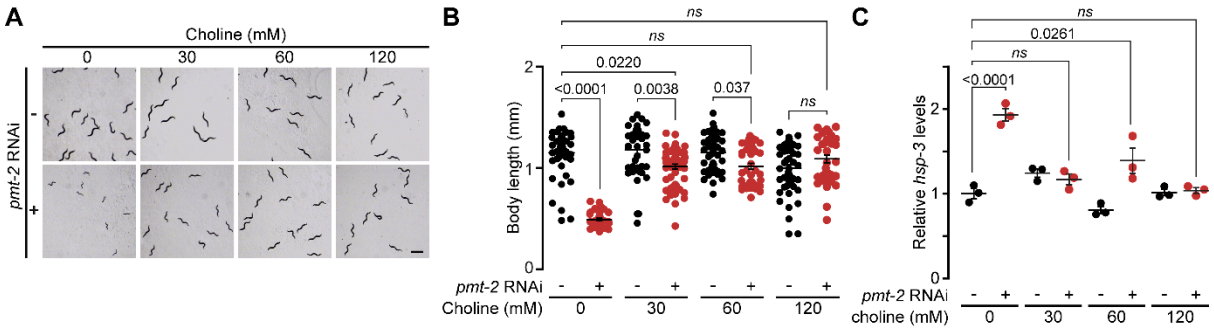

Figure S1, Refers to **Figure 1**. **Choline supplementation restores developmental defects in *pmt-2(RNAi)* animals.**
(A) Representative choline rescue assay of *pmt-2(RNAi)* developmental defect. L1 worms were grown on *pmt-2* RNAi or empty vector on plates supplemented with 0, 30, 60, or 120 mM choline, and images were taken after 48 h. Scale bar, 100 µm. (B) Body length quantification of worms from **A**. WT, 0 mM choline, n=47(-), n=32(+); 30 mM choline, n=39(-), n=58(+); 60 mM choline, n=48(-), n=43(+); 120 mM choline, n=54(-), n=38(+). (C) qPCR of *hsp-3* expression level in WT worms treated as in **A**. Data shown is the mean ± s.e.m. of at least three independent experiments. Statistical analysis was subjected to one-way ANOVA followed by Tukey's multiple comparisons adjustment. ns, non-significant.

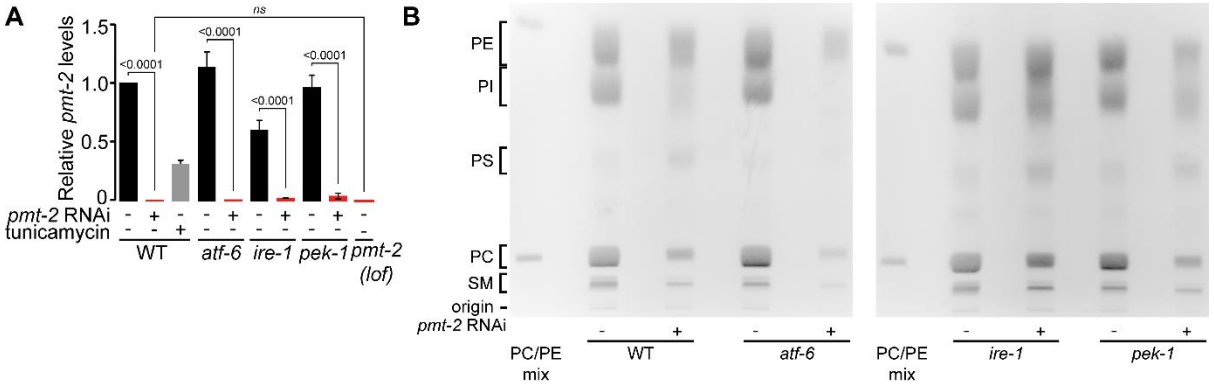

Figure S2, Refers to **Figure 2A-B**. **Inactivation of *pmt-2* decreased PC content in worms.**
(A) qPCR of *pmt-2* expression after *pmt-2* RNAi treatment in WT, *atf-6(lof)*, *ire-1(lof),* and *pek-1(lof)* worms. *pmt-2(lof)* worms were used as a control. *pmt-2* RNAi treatment efficiently silenced expression of *pmt-2* across all the strains tested. (B) Representative separation of PE, MMPE, DMPE, and PC from total lipid extract using thin-layer chromatography (TLC). Comparison of phospholipid levels in WT, *atf-6(lof)*, *ire-1(lof)* and *pek-1(lof)* animals treated with *pmt-2* RNAi. POPE (1-palmitoyl-2-oleoyl-sn-glycero-3-phosphoethanolamine; 16:0-18:1n9 PE) and DOPC (1,2-dioleoyl-sn-glycero-3-phosphocholine; 18:1n9 PC) were used as markers. Data shown is the mean ± s.e.m. of at least three independent experiments. Statistical analysis was subjected to one-way ANOVA followed by Tukey's multiple comparisons adjustment. ns, non-significant.

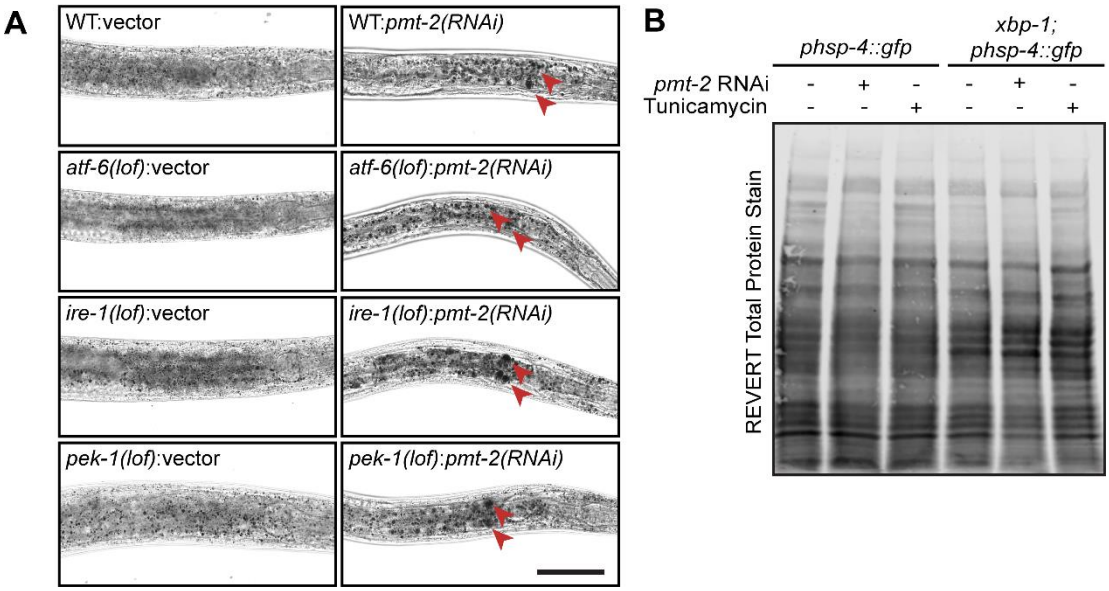

Figure S3, Refers to **Figure 2C,F**. **Lipid perturbation induces lipid droplets accumulation and activates the UPR.**
(A) Representative images of lipid droplet visualised using Sudan Black B staining of WT, *atf-6(lof)*, *ire-1(lof)* and *pek-1(lof)* animals treated with *pmt-2* RNAi. Brightfield images of stained worms are shown using 63X objective lens. Red arrowhead highlights large LDs. Scale bar, 100 µm. (B) Total protein stain verified equal loading and served as normalization control for the immunoblot.

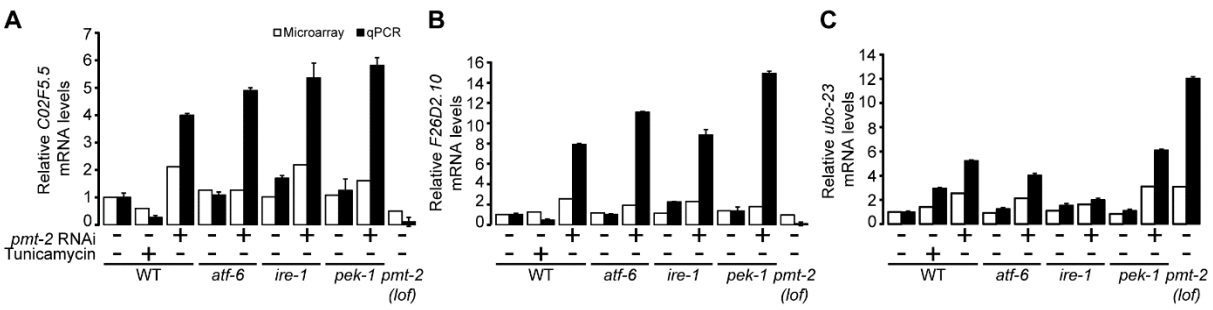

Figure S4, Refers to **Figure 3**. **Validation of DNA microarray analysis using quantitative real-time PCR.**
(A-C) Comparison of *C02F5.5* (A), *F26D2.10* (B), and *ubc-23* (C) gene expression in WT, *atf-6(lof)*, *ire-1(lof)* and *pek-1(lof)* animals treated with *pmt-2* RNAi by DNA microarray (white bars) and qPCR (black bars). *C02F5.5* and *F26D2.10*, are both uncharacterized genes; *ubc-23*, a member of the BCL-2 family. The figure represents technical triplicates.

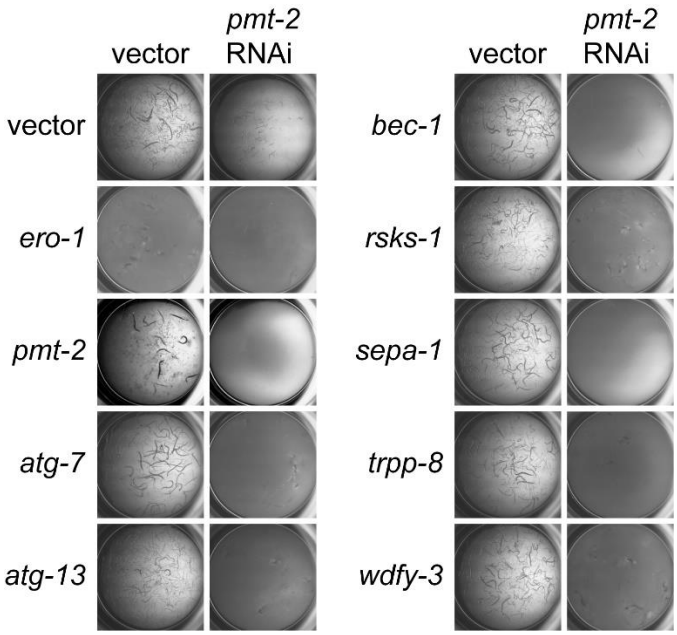

Figure S5, Refers to Figure 5. **Autophagy is essential during lipid perturbation.** WT worms were treated with vector or *pmt-2* RNAi for 36 h and subsequently subjected to RNAi in liquid media in a 96-well plate for 5 days. The worms were scored based on their developmental defects as described in Fig. 5A. *ero-1* RNAi was included as a positive control.

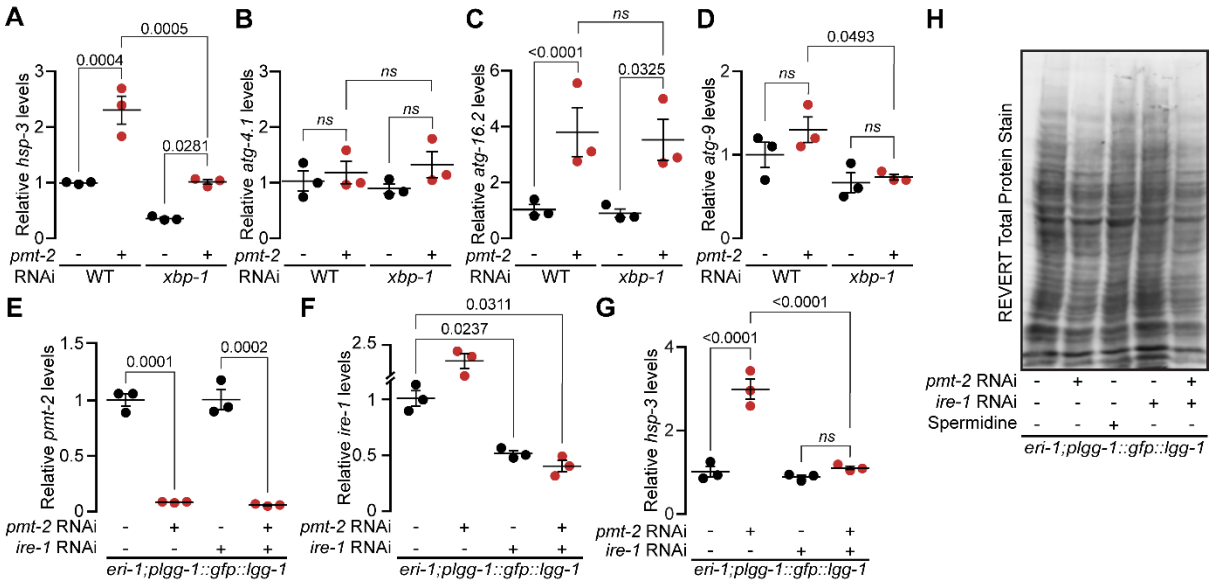

Figure S6, Refers to Figure 5. **Autophagy is partially dependent on XBP-1**. qPCR comparing expression of *hsp-3* (A), *atg-4.1* (B), *atg-16.2* (C), *atg-9* (D) in WT and *xbp-1(lof)* mutants treated with *pmt-2* RNAi. qPCR comparing expression of *pmt-2* (E), *ire-1* (F), *hsp-3* (G) in *eri-1;plgg-1::gfp::lgg-1* worms treated with *pmt-2, ire-1*, and *ire-1:pmt-2* RNAis; technical triplicates. (H) Total protein stain verified equal loading and served as normalization control for the immunoblot. Data shown is the mean ± s.e.m. of at least three independent experiments. Statistical analysis was subjected to one-way ANOVA followed by Tukey's multiple comparisons adjustment. ns, non-significant.

Table S1. Oligonucleotide primers used in the study.

Gene	Sequence (5' to 3')	Assay
act-1	AGGACTGGGTGCTCTTCTGG GAGCACGGTATCGTCACCAA	qPCR
atg-4.1	AGGAAGATGGAATCGAGGCAA TGCAACCCCATCCTTGATCC	qPCR
atg-9	ATGGAATCGTTCTTCTCACTG GCAGGAGGTATTGTATCTTCTC	qPCR
atg-16.2	ATGTGCTGGCTGGATCTTCG GAGCCGAATCTGATCTCGCAG	qPCR
atg-18	CCGAAGTCAGACACTAGTCGAG TCGGAACCGATTGGTTGCTTG	qPCR
bec-1	AAGCTCTGACTGGACATTCTCG GCGTCAGAGCAATCATTACAAAC	qPCR
atg-18	CCGAAGTCAGACACTAGTCGAG TCGGAACCGATTGGTTGCTTG	qPCR
C02F5.5	CATCTTTTGAGCTTATGATGGTGCT AAGCACCAAGGAACACGAGAT	qPCR
epg-4	CCAATTCCTCTTATCACACCA GTCGAAGAAGTAATCGAAACAG	qPCR
F26D2.10	CTCTTGTGGCAGCTCATGGT CGTGGATCAAAAACAGCGGC	qPCR
hsp-3	AGAAGGAGACCAAGTATGGAACC TGATACGGTTTCCTTGGTCGTT	qPCR
hsp-4	CATCTCGTGGAATCAACCCT TGACGTCAAGAAGGACAACA	qPCR
lgg-1	TCGTGATGGTCCTGGTAGAGT ACGCATCCAACTTCGTCCA	qPCR
ire-1	ACAATGGCTAGTCAGCGAGG CAATCCAGCCATCGGTTCCT	qPCR
pmt-2	AGAACGTGGTCATTTGGAGCAG TTCGCGTTGGGTAAACTTCGAC	qPCR

Table S2, Refers to **Figure 3A**. **List of upregulated and downregulated genes in *pmt-2(RNAi)* and WT treated with tunicamycin compared to WT animals.** Excel Spreadsheet

Click here to Download Table S2

Table S3, Refers to **Figure 3B**. **List of upregulated genes from the four-way Venn diagram.** Excel Spreadsheet

Click here to Download Table S3

Table S4, Refers to **Figure 3C**. **Hierarchical clustering gene list.** Excel Spreadsheet

Click here to Download Table S4

Table S5, Refers to **Figure 4**. **Predominant GO terms of each cluster.** Excel Spreadsheet

Click here to Download Table S5

Table S6, Refers to **Figure 5**. **Phenotype from RNAi screen of autophagy genes.** Excel Spreadsheet

Click here to Download Table S6